Acta Pharmaceutica Sinica B 2020;10(3):462–474

Chinese Pharmaceutical Association
Institute of Materia Medica, Chinese Academy of Medical Sciences

Acta Pharmaceutica Sinica B

www.elsevier.com/locate/apsb
www.sciencedirect.com

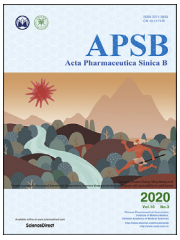

ORIGINAL ARTICLE

Benzydamine inhibits osteoclast differentiation and bone resorption *via* down-regulation of interleukin-1β expression

Han Saem Son[†], Jiae Lee[†], Hye In Lee, Narae Kim, You-Jin Jo, Gong-Rak Lee, Seong-Eun Hong, Minjeong Kwon, Nam Young Kim, Hyun Jin Kim, Jin Ha Park, Soo Young Lee, Woojin Jeong[*]

Department of Life Science and the Research Center for Cellular Homeostasis, Ewha Womans University, Seoul 03760, South Korea

Received 4 March 2019; received in revised form 23 September 2019; accepted 25 October 2019

KEY WORDS

Benzydamine;
Osteoclast;
Bone;
Interleukin-1β;
Nuclear factor-κB;
Activator protein-1

Abstract Bone diseases such as osteoporosis and periodontitis are induced by excessive osteoclastic activity, which is closely associated with inflammation. Benzydamine (BA) has been used as a cytokine-suppressive or non-steroidal anti-inflammatory drug that inhibits the production of pro-inflammatory cytokines or prostaglandins. However, its role in osteoclast differentiation and function remains unknown. Here, we explored the role of BA in regulating osteoclast differentiation and elucidated the underlying mechanism. BA inhibited osteoclast differentiation and strongly suppressed interleukin-1β (IL-1β) production. BA inhibited osteoclast formation and bone resorption when added to bone marrow-derived macrophages and differentiated osteoclasts, and the inhibitory effect was reversed by IL-1β treatment. The reporter assay and the inhibitor study of IL-1β transcription suggested that BA inhibited nuclear factor-κB and activator protein-1 by regulating IκB kinase, extracellular signal regulated kinase and P38, resulting in the down-regulation of IL-1β expression. BA also promoted osteoblast differentiation. Furthermore, BA protected lipopolysaccharide- and ovariectomy-induced bone loss in mice, suggesting therapeutic potential against inflammation-induced bone diseases and postmenopausal osteoporosis.

*Corresponding author. Tel.: +82 2 3277 4495; fax: +82 2 3277 3760.
E-mail address: jeongw@ewha.ac.kr (Woojin Jeong).
[†]These authors made equal contributions to this work.
Peer review under responsibility of Chinese Pharmaceutical Association and Institute of Materia Medica, Chinese Academy of Medical Sciences

https://doi.org/10.1016/j.apsb.2019.11.004

1. Introduction

Bone homeostasis is maintained by the balanced action of bone-forming cells known as osteoblasts and bone-resorbing cells known as osteoclasts[1,2]. Abnormal osteoclast formation and activity has been recognized as a major cause of bone diseases such as osteoporosis, rheumatoid arthritis and periodontitis[3,4]. The therapeutic strategy against these diseases has been focused primarily on the inhibition of osteoclast differentiation and function. Therefore, the development of a new agent that regulates osteoclast differentiation and activity has therapeutic implications[5–7].

Osteoclast is a giant multinucleated cell that is differentiated from hematopoietic stem cell by the cooperative action of macrophage-colony stimulating factor (M-CSF) and receptor activator of NF-κB ligand (RANKL)[8]. RANKL binds to its receptor, RANK and activates tumor necrosis factor (TNF) receptor-associated factor 6 (TRAF6), which in turn acts as an adapter in the downstream signaling pathways[9]. Activated TRAF6 induces the stimulation of NF-κB and mitogen-activated protein kinases (MAPKs) including c-Jun N-terminal kinase (JNK), extracellular signal-regulated kinase (ERK), and P38[10–12]. In addition, c-FOS, a member of the activator protein-1 (AP-1) transcription factor family is induced[13,14]. Both NF-κB and AP-1 induce the initial expression of nuclear factor of activated T-cells, cytoplasmic 1 (NFATc1), a master regulator of osteoclastogenesis[15,16]. NFATc1 is auto-amplified and regulates the expression of osteoclast-specific genes such as tartarate-resident alkaline phosphatase (TRAP), matrix metalloprotease 9 (MMP9), and cathepsin K (CTSK) in conjunction with other transcription factors such as NF-κB and AP-1[17].

NF-κB and AP-1 regulate the production of pro-inflammatory cytokines including interleukins (IL)-1β, IL-6 and TNFα, and prostaglandin E2 (PGE2)[18], which trigger inflammation in activated macrophages[19,20]. IL-1β, IL-6, TNFα and PGE2 promote osteoclast differentiation *via* a RANKL-independent mechanism[21,22]. Therefore, these pro-inflammatory cytokines represent potent stimulators of osteoclastic bone resorption in inflammatory bone diseases including osteoporosis, periodontal disease, and rheumatoid arthritis[22–24].

Benzydamine (BA) is currently used to reduce fever and pain as an anti-inflammatory drug with local analgesic and anesthetic properties[25]. BA has been known to act as a non-steroidal anti-inflammatory drug that inhibits prostaglandin synthesis or as a cytokine-suppressive anti-inflammatory drug to suppress pro-inflammatory cytokine production[26]. In this study, we demonstrated the role of BA as an inhibitor of osteoclast differentiation and bone resorption. Furthermore, we highlighted the therapeutic potential of BA in bone diseases using mouse models of inflammation- and ovariectomy-induced bone destruction.

2. Materials and methods

2.1. Reagents and antibodies

Recombinant human M-CSF and mouse RANKL proteins were prepared as previously described[5]. BA was purchased from AK Scientific, Inc. (Union City, CA, USA) and recombinant human IL-1β was supplied by R&D systems, Inc. (Minneapolis, MN, USA). PGE2 was purchased from Cayman Chemical (Ann Arbor, MI, USA). Lipopolysaccharide (LPS), U0126 and SC-514 were supplied by MilliporeSigma (Burlington, MA, USA). SB202190 and SP600125 were supplied by AG Scientific, Inc. (San Diego, CA, USA). A rabbit polyclonal antibody against β-actin was purchased from Abcam (Cambridge, MA, USA). Rabbit polyclonal antibodies against phosphorylated (p-)IκBα, p-JNK, p-ERK and p-P38, and a rabbit monoclonal antibody against p-p65 were purchased from Cell Signaling Technology (Danvers, MA, USA). A goat polyclonal anti-mouse secondary antibody (Alexa Fluor 546 conjugate) was purchased from Thermo Fisher Scientific (Waltham, MA, USA). Rabbit polyclonal antibodies against IκBα, JNK1, P38 and c-FOS, and mouse monoclonal antibodies against NFATc1, p65, ERK2, CTSK and integrin β_3 were procured from Santa Cruz Biotechnology (Dallas, TX, USA). A rabbit polyclonal antibody against superoxide dismutase 2 (SOD2) was purchased from Upstate Biotechnology (Lake Placid, NY, USA). A rabbit monoclonal antibody against ATP6V0D2 was kindly provided by Dr. SY Lee (Ewha Womans Univ. Seoul, Korea).

2.2. Preparation of bone marrow-derived macrophages

Bone marrow-derived macrophages (BMMs) were prepared as osteoclast precursor cells as previously described[27]. Bone marrow cells were flushed from the femurs and tibiae of 8-week-old C57BL/6 male mice using α-minimum essential medium (α-MEM) containing 10% fetal bovine serum (FBS), 100 U/mL penicillin and 100 μg/mL streptomycin, followed by incubation at 37 °C for 1 day. Nonadherent cells were harvested and incubated in Gey's solution for 10 min to remove red blood cells. After clarification by centrifugation at 1000 rpm, the cells were cultured in α-MEM containing 10% FBS, 100 U/mL penicillin, 100 μg/mL streptomycin and 50 ng/mL M-CSF for 3 days. Adherent cells were used as osteoclast precursors.

2.3. Osteoclast differentiation and TRAP staining

BMMs were incubated in α-MEM containing 10% FBS, 40 ng/mL M-CSF and 50 ng/mL RANKL for 3–5 days. After osteoclast differentiation, the cells were washed with phosphate-buffered saline (PBS), fixed for 10 min with 4% paraformaldehyde and stained for TRAP using a leukocyte acid phosphatase cytochemistry kit (MilliporeSigma) according to the manufacturer's instructions. TRAP-positive multinucleated cells containing three or more nuclei were counted as osteoclasts under a light microscope (Nikon, Shinagawa, Tokyo, Japan).

2.4. Actin-ring staining

Cells were fixed with 3.7% formaldehyde solution in PBS, permeabilized with 0.1% Triton X-100, and incubated with Alexa Fluor 488-phalloidin (Thermo Fisher Scientific, Waltham, MA, USA). After washing with PBS, the cells were treated with 4′,6-diamidino-2-phenylindole (Roche, Basel, Switzerland) and then photographed under a fluorescence microscope (Carl Zeiss, Oberkochen, Germany).

2.5. Bone resorption assay

BMMs were plated on dentin discs (Immunodiagnostic Systems, Boldon Colliery, Tyne and Wear, UK) and treated with 40 ng/mL M-CSF and 50 ng/mL RANKL for 12 days. The cells were completely removed from the dentin discs *via* abrasion with a cotton tip. The dentin discs were stained with hematoxylin. The

resorption pits were imaged under a light microscope at 100 × magnification and their areas were determined *via* Image-Pro Plus 4.5 software (Media Cybernetics, Rockville, MD, USA).

2.6. *RNA isolation, reverse transcription, and real-time PCR*

Total RNA was isolated using the TRIzol reagent (Thermo Fisher Scientific) according to the manufacturer's instructions and quantified by measuring the absorbance at 260 nm. The total RNA (2 μg) was incubated with 0.5 μg of oligo (dT) primer at 70 °C for 5 min and cooled immediately on ice. The first-strand cDNA was synthesized by the addition of 200 units of M-MLV reverse transcriptase (Promega, Madison, WI, USA), 24 units of ribonuclease inhibitor and 0.25 mmol/L of each dNTP, followed by incubation for 1 h at 42 °C, and enzyme inactivation at 70 °C for 10 min. The cDNA was amplified in a reaction mixture containing SYBR Green PCR Master Mix (Bioline, Taunton, MA, USA) and 1 μmol/L gene-specific primer using a StepOnePlus real-time PCR (Applied Biosystems, Foster City, CA, USA). The amplification protocol consisted of an initial step of 2 min at 50 °C and 2 min at 95 °C followed by 40 cycles of 15 s at 95 °C and 1 min at 60 °C. Each mRNA level was normalized to actin level. The primers used in the current study were as follows: *Nfatc1* (5′-CTTCAGCTGGAGGACACC-3′ and 5′-CCAATGAACAGCTGTAGCG-3′), *Acp5* (5′-CCAGCGACAAGAGGTTCC-3′ and 5′-AGAGACGTTGCCAAGGTGAT-3′), *Mmp9* (5′-AGACGACAT

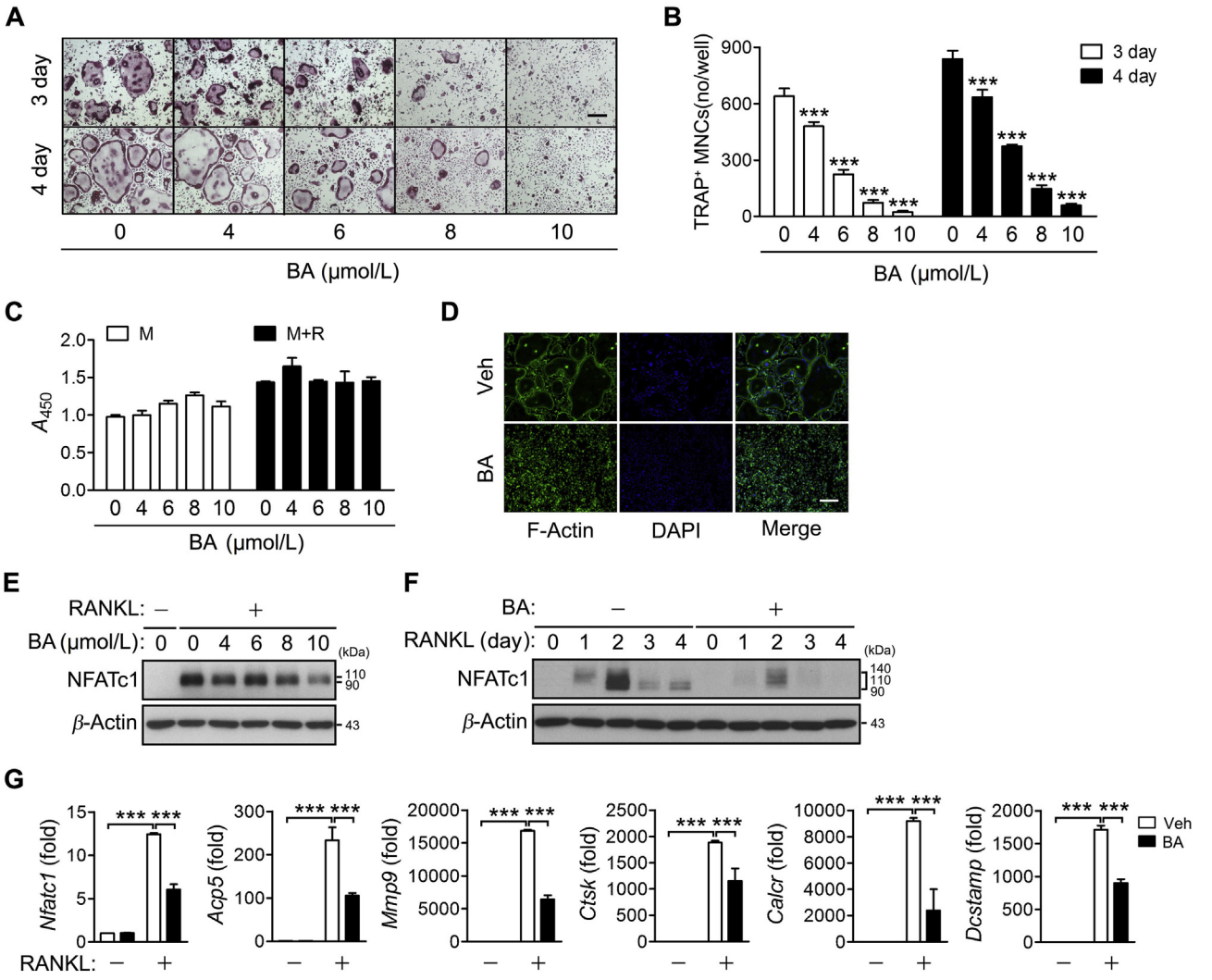

Figure 1 Inhibition of RANKL-induced osteoclast differentiation and NFATc1 expression by BA. BMMs were cultured in the presence of M-CSF and were treated with RANKL in the presence of the indicated concentrations of BA for 3 and 4 days (A) and (B), 4 days (C) or 2 days (E), and in the presence of 10 μmol/L BA for 2 days (G), 4 days (D) or the indicated times (F). (A) The cells were fixed, subjected to TRAP staining and visualized under a light microscope. Scale bar, 200 μm. (B) TRAP-positive multinucleated cells (MNCs) were counted. $^{***}P < 0.001$ control *vs*. BA. (C) The cell viability assay was performed using the WST-1 reagent. The percentage of viable cells was calculated based on the absorbance of the sample relative to positive control at 450 nm. M, M-CSF only; M + R, M-CSF plus RANKL. $^{*}P < 0.05$, $^{***}P < 0.001$ control *vs*. BA. (D) The cells were stained with Alexa Fluor 488-phalloidin and DAPI, and then photographed under a fluorescence microscope. Scale bar, 200 μm. (E) and (F) The expression of NFATc1 was analyzed by immunoblotting. (G) Real-time PCR was performed to quantify the mRNA levels of *Nfatc1* and its target genes. Relative levels of individual mRNA were normalized to those of β-actin mRNA and presented as fold induction. Veh, vehicle. $^{***}P < 0.001$ between the indicated groups.

AGACGGCATC-3′ and 5′-TGCTGTCGGCTGTGGTTC-3′), *Ctsk* (5′-ACCACTGCCTTCCAATACG-3′ and 5′-CGTGGCGTTA TACATACAAC-3′), *Calcr* (5′-TGATGACTCTCAGGACAATG-3′ and 5′-ACTGGATCAATCTGTAGGAG-3′), *Dcstamp* (5′-TTAT GTGTTTCCACGAAGCCCTA-3′ and 5′-ACAGAAGAGAG CAGGGCAACG-3′), *Il1b* (5′-CTGGTGTGTGACGTTCC-CATTA-3′ and 5′-CCGACAGCGAGGCTTT-3′), *Il6* (5′-GTTGCCTTCTTGGGACTGATG-3′ and 5′-GCCATTGCACAA CTCTTTTCTC-3′), *Tnf* (5′-CCCTCACACTCAGATCATCTTCT-3′ and 5′-GCTACGACGTGGGCTACAG-3′), *Pla2* (5′-CAGCA-CATTATAGTGGAACACCA-3′ and 5′-GTCCAGCATATCGCCA AAGGT-3′) *Cox2* (5′-GATCATAAGCGAGGACCTG-3′ and 5′-GTCTGTCCAGAGTTTCACC-3′), *Ptges* (5′-GCACACTGCTG GTCATCAAGA-3′ and 5′-AGCCGAGGAAGAGGAAAGGAT-3′), *Sod2* (5′-ATTAACGCGCAGATCATGCA-3′ and 5′-TGTCC CCCACCATTGAACTT-3′), *Fos* (5′- GAGAAACGGAGAATCC GAAG-3′ and 5′- GAGAAACGGAGAATCCGAAG-3′), *Atp6 v0d2* (5′-CAGAGATGGAAGCTGT-3′ and 5′-TGCCAAATGAG TTCAG-3′), *Itgb3* (5′-GGAGTGGCTGATCCAGATGT-3′ and 5′-TCTGACCATCTTCCCTGTCC-3′), *Actb* (5′-ACCCTAAGGC-CAACCGTG-3′ and 5′-GCCTGGATGGCTACGTAC-3′), *Runx2* (5′-TGCCTTCAGCACCCTATACC-3′ and 5′-AGGTTGG AGGCACACATAGG-3′), *Sp7* (5′-AGCGACCACTTGAGCAA ACAT-3′ and 5′-GCGGCTGATTGGCTTCTTCT-3′), and *Msx2* (5′-CTACCCGTTCCATAGACCTGTGCTT-3′ and 5′-GAGAGG-GAGAGGAAACCCTTTGAA-3′). Melting curve analysis was performed to ensure a single PCR product.

2.7. Determination of IL-1β levels

BMMs or osteoclasts were incubated with 40 ng/mL M-CSF and 50 ng/mL RANKL in the absence or presence of 10 μmol/L BA for 2 days. The levels of IL-1β in the culture medium were determined using a mouse IL-1β/IL-1F2 Quantikine ELISA Kit (R&D Systems, Inc.) according to the manufacturer's instructions.

2.8. Transfection and luciferase reporter assay

RAW264.7 cells were transfected for 24 h with 0.45 μg of luciferase reporter plasmid and 0.15 μg of pRLSV40 (internal control) in a 24-well plate using Lipofectamine 3000 reagent (Thermo Fisher Scientific) according to the manufacturer's instructions. A dual luciferase assay (Promega, Fitchburg, WI, USA) was subsequently performed. The activity of firefly luciferase was

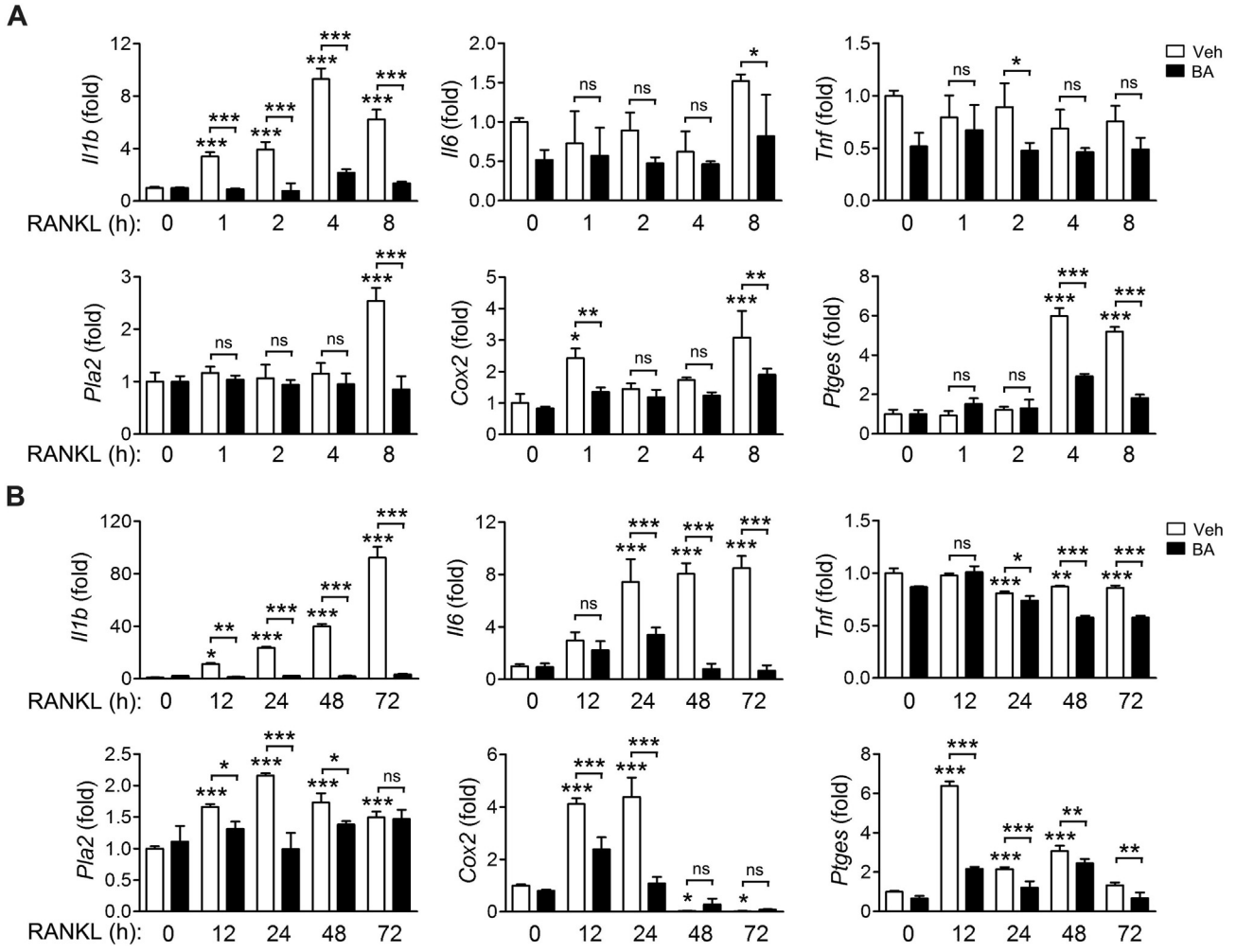

Figure 2 Regulation of the expression of pro-inflammatory cytokines and genes related to PGE2 synthesis by BA in 0-8 h (A) and 12-72 h (B). BMMs were cultured in the presence of M-CSF and were treated with RANKL in the presence of 10 μmol/L BA for the indicated times (A, the early stage; B, the late stage). The mRNA level of individual genes was determined by real-time PCR and presented as fold induction. $^{*}P < 0.05$, $^{**}P < 0.01$ and $^{***}P < 0.001$ control *vs*. RANKL in the absence of BA or between the indicated groups. ns, not significant.

normalized to that of the *Renilla* enzyme and was expressed as a fold increase relative to the normalized value of control cells.

2.9. Osteoblast differentiation and mineralization

The calvaria of 2-day-old C57BL/6 mice were dissected, and digested with 0.03% collagenase I and 0.2% dispase for 4 h. The isolated cells were cultured in α-MEM containing 10% FBS, 100 U/mL penicillin, and 100 mg/mL streptomycin. Calvaria cells were cultured in osteogenic media (OGM), α-MEM containing 0.1 μmol/L dexamethasone, 10 mmol/L β-glycerophosphate, and 50 μg/mL ascorbic acid for 12 days. The cells were fixed in 4% paraformaldehyde and incubated with a solution containing 0.1 mg/mL naphthol AS-MX phosphate, 0.5% *N*,*N*-dimethyl formamide and 0.6 mg/mL fast blue BB salt for alkaline phosphatase (ALP) staining. To measure ALP activity, cell lysates were incubated with 5 m mol/L *p*-nitrophenyl phosphate for 60 min, and the released amount of *p*-nitrophenol was determined by measuring the absorbance at 405 nm using a microplate reader (Biotek, Winooski, VT, USA). After incubation with OGM for 21 days, the cells are fixed in 4% paraformaldehyde and stained with 2% alizarin red S (ARS) solution for 40 min at room temperature. The bound ARS was dissolved in 10% cetylpyridinium chloride and the absorbance was measured at 545 nm. All the reagents used in these experiments were purchased from MilliporeSigma.

2.10. Calvarial injection of LPS and histological analysis

Eight-week-old C57BL/6 male mice were randomly divided into the following groups ($n = 5$ per group): PBS control, LPS, and LPS plus BA. LPS (12.5 mg/kg body weight) alone or combined with BA (10 mg/kg), each in a 100-μL PBS, was injected into the space between the subcutaneous tissue and the periosteum of the skulls in mice on days 0 and 2. The mice were killed in a CO_2 chamber 5 days after the first injection. The calvariae were dissected and fixed with 4% paraformaldehyde at room temperature overnight. The specimens were washed with PBS and decalcified with 0.5 mol/L ethylenediaminetetraacetic acid for 5 days, embedded in low-melting paraffin, cut into 4-μm sections, and stained with TRAP and hematoxylin.

2.11. Ovariectomy and micro-computed tomography imaging

Ovariectomy (OVX) and micro-computed tomography were carried out as previously described[28]. Eight-week-old C57BL/6 female mice were randomized into the following groups ($n = 5$ in each group): sham operation, OVX, and OVX followed by BA treatment. A week after surgery, BA (10 mg/kg) was injected intraperitoneally six times a week for three weeks. The tibiae were decalcified and embedded in paraffin. Bone sections were stained with TRAP and hematoxylin, and TRAP-positive osteoclasts were quantified using Image-Pro Plus 4.5 software (Media Cybernetics). The femurs were evaluated using micro-computed tomography (Bruker, Kontich, Belgium).

2.12. Animal care

All mice were allowed free access to food and water, and caged under a 12-h light/12-h dark cycle. All animal studies were conducted in accordance with the protocols approved by the International Animal Care and Use Committee of Ewha Womans University (Korea).

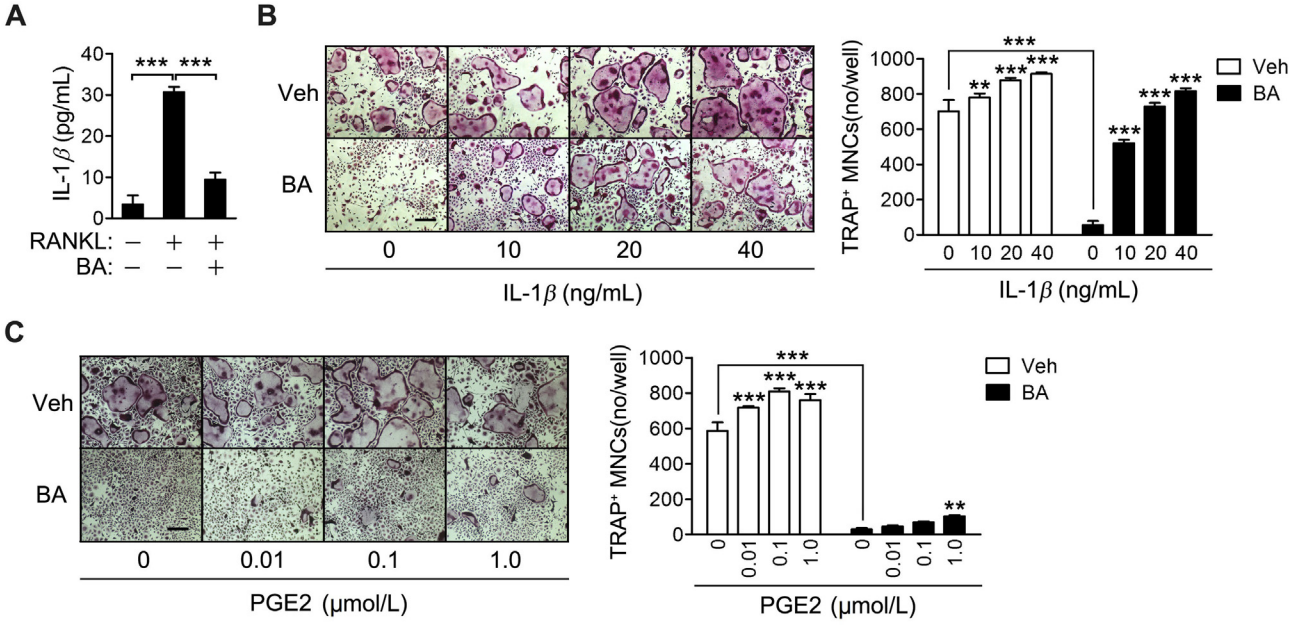

Figure 3 Reversal of BA inhibition of osteoclast differentiation by IL-1β treatment. (A) BMMs were cultured in the presence of M-CSF and were incubated with RANKL for 2 days in the presence of 10 μmol/L BA. The amount of IL-1β in the culture media was determined by ELISA. (B) and (C) BMMs were cultured in the presence of M-CSF and were exposed to RANKL in the presence of 10 μmol/L BA and the indicated concentrations of IL-1β (B) or PGE2 (C). The cells were fixed, subjected to TRAP staining and observed under a light microscope. Scale bar, 200 μm. TRAP-positive MNCs were counted. $^{**}P < 0.01$ and $^{***}P < 0.001$ control *vs*. IL-1β (B) or control vs PGE2 (C) in the absence and presence of BA, or between the indicated groups.

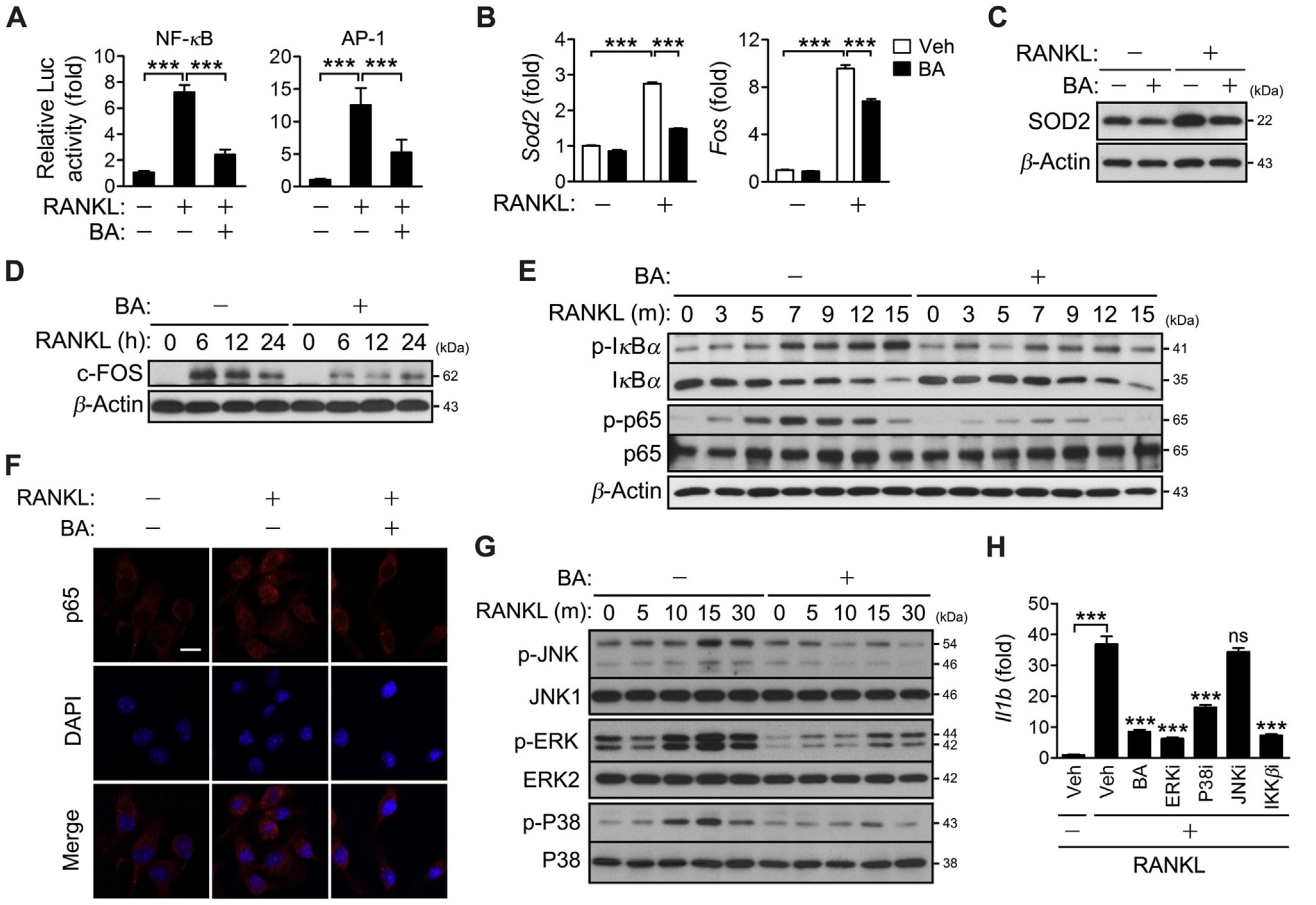

Figure 4 BA inhibition of IL-1β expression *via* down-regulation of IKK, ERK and P38. (A) RAW264.7 cells were transfected for 24 h with 0.45 μg of pNF-κB-Luc (NF-κB reporter plasmid) or pAP-1-Luc (AP-1 reporter plasmid) and 0.15 μg of pRL-SV40 (internal control). The cells were treated with RANKL for 24 h in the absence or presence of 10 μmol/L BA. The luciferase activity of each cell lysate was measured using a dual-luciferase assay system. The activity of firefly luciferase was normalized to that of the *Renilla* enzyme and expressed as fold increase relative to the activity of RANKL-untreated cells. (B−H) BMMs were cultured in the presence of M-CSF and were treated with RANKL for 24 h (B and C), the indicated times (D, E and G), 15 min (F) and 48 h (H) in presence of 10 μmol/L BA or 10 μmol/L inhibitors of ERK (U0126), P38 (SB202190), JNK (SP600125) and IKK (SC-514) (G). Cell lysates were subjected to immunoblotting analysis (C−E and G). The cells were stained with p65 antibody and DAPI, and then photographed under a fluorescence microscope. Scale bar, 10 μm (F). The transcription of individual genes was quantified by real-time PCR and presented as fold induction (B and H). $^{***}P < 0.001$ between the indicated groups (A, B and H) or vehicle *vs*. inhibitors in the presence of RANKL (H). ns, not significant.

2.13. Statistical analysis

Data are presented as the mean ± standard deviation of the mean (SD). Unless otherwise indicated, $n = 3$. Statistical significance was determined by the one-way or two-way analysis of variance (ANOVA) using the Prism software version 5.0 (GraphPad, San Diego, CA, USA). The P values less than 0.05 were considered statistically significant.

3. Results

3.1. BA inhibits RANKL-induced osteoclast differentiation and NFATc1 activation

BA has been used as an anti-inflammatory drug to inhibit the synthesis of pro-inflammatory cytokines and prostaglandins, which are known to promote osteoclast differentiation. Thus, we investigated the role of BA in osteoclast differentiation. During the RANKL-induced differentiation of BMMs to osteoclasts, BA inhibited osteoclast formation in a dose-dependent manner (Fig. 1A and B), without affecting the cell viability at the concentrations tested (Fig. 1C). Also, BA strongly inhibited actin ring formation (Fig. 1D).

To further validate the BA inhibition of osteoclast differentiation and to determine its effective concentration for subsequent experiments, the concentration-dependent effect of BA on NFATc1 expression was examined. Incubation of BMMs with RANKL for 2 days in the presence of various concentrations of BA resulted in a significant inhibition of NFATc1 expression at 10 μmol/L BA (Fig. 1E). The NFATc1 inhibition was sustained for 4 days (Fig. 1F). BA also significantly inhibited the transcription of *Nfatc1* and its target genes including *Acp5*, *Mmp9*, *Ctsk*, *Calcr* and *Dcstamp* (Fig. 1G). Thus, 10 μmol/L BA was used in the subsequent *in vitro* experiments.

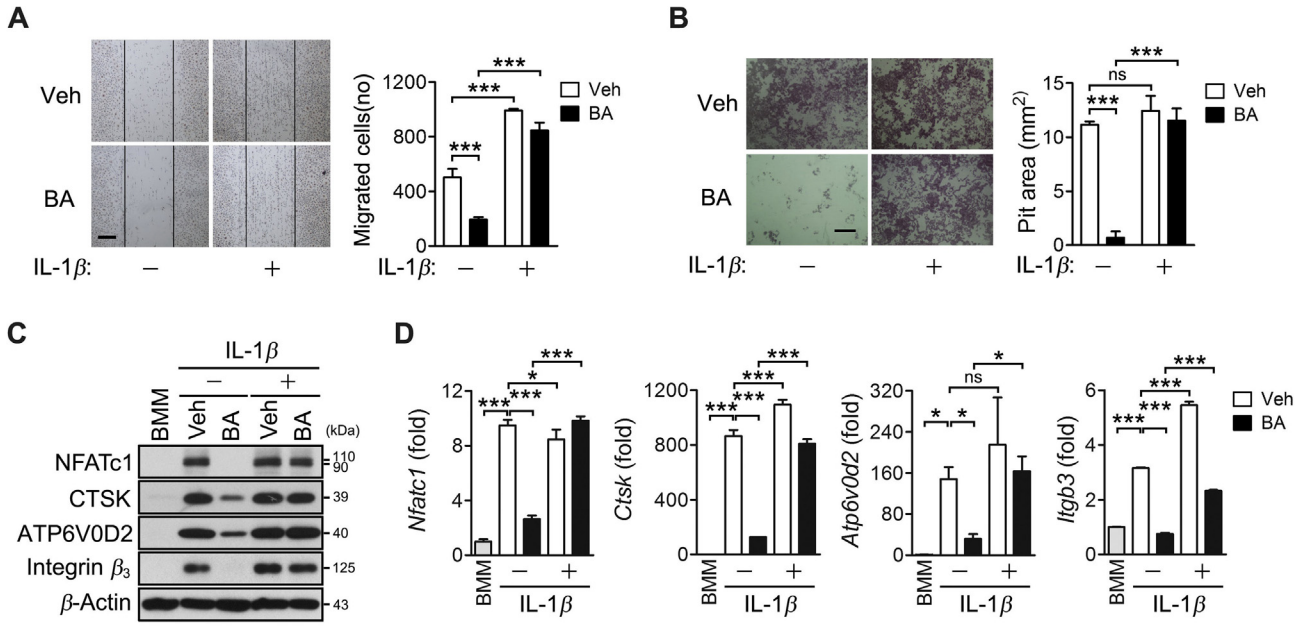

Figure 5 BA inhibition of cell migration and bone resorption, and their rescue by IL-1β treatment. (A) BMMs were cultured in the presence of M-CSF and were further incubated with RANKL for 15 h after gentle scratching in the absence and presence of 10 μmol/L BA or IL-1β (20 ng/mL). The cells migrating to the scratched area were counted. (B−D) BMMs were cultured in the presence of M-CSF and were treated with RANKL for 12 days on dentin discs (B) or 2 days (C and D). The cells were removed from the dentin discs and the resorption pits were visualized by staining with hematoxylin (B). The cell lysates were subjected to immunoblotting analysis (C). The individual gene transcription was quantified by real-time PCR and presented as fold induction (D). Scale bar, 200 μm $^{*}P < 0.05$ and $^{***}P < 0.001$ between the indicated groups. ns, not significant.

3.2. BA inhibits RANKL-induced pro-inflammatory cytokine expression and PGE2 synthesis

BA is known to suppress pro-inflammatory cytokine expression and PGE2 synthesis. Thus, we measured the transcriptional expression of pro-inflammatory cytokine genes including *Il1b*, *Il6* and *Tnf*, and the PGE2 synthesis-related genes including *Pla2*, *Cox2* and *Ptges* at various time points after the stimulation of BMMs with RANKL in the presence of BA. The expression of *Il1b* gene was induced very early, sustained during the incubation period and was strongly suppressed by BA (Fig. 2A). However, *Il6* and *Tnf* genes were not expressed initially upon RANKL treatment (Fig. 2A). The genes *Pla2* and *Ptges* were slightly induced at 4−8 h after RANKL exposure and their expression was inhibited by BA (Fig. 2A). The expression of *Il1b* and *Il6* genes was induced in the late stages of RANKL treatment; their expression was significantly inhibited by BA; however, *Tnf* was not expressed (Fig. 2B). The genes *Cox2* and *Ptges* were expressed at 12−24 h after RANKL treatment, which was inhibited by BA (Fig. 2B). Taken together, IL-1β may be a predominant inflammatory molecule that is strongly and consistently expressed at all the times following RANKL treatment, and is effectively regulated by BA.

3.3. IL-1β treatment reverses BA inhibition of osteoclast differentiation

The amount of IL-1β protein secreted into culture media was also strongly increased by RANKL treatment and was significantly reduced by BA, based on ELISA results (Fig. 3A). The role of BA in the inhibition of osteoclast differentiation by suppressing IL-1β or PGE2 production, was investigated by analyzing the effect of IL-1β and PGE2 on RANKL-induced osteoclast differentiation in the absence or presence of BA. IL-1β significantly increased osteoclast formation in vehicle control and effectively rescued the osteoclast differentiation inhibited by BA (Fig. 3B). PGE2 also reversed BA inhibition of osteoclast differentiation in a dose-dependent manner; however, it had a marginal effect (Fig. 3C). These results indicate that BA may inhibit osteoclast differentiation by suppressing RANK-induced IL-1β production.

3.4. BA inhibits NF-κB and AP-1-dependent IL-1β expression via down-regulation of IKK, ERK and P38

The regulatory role of BA in IL-1β expression was explored. The IL-1β promotor carries a single NF-κB binding site, two AP-1 binding sites and one serum responsive element[29], and the expression of IL-1β is regulated *via* NF-κB and AP-1[30,31]. Thus, the effect of BA on RANKL-induced NF-κB and AP-1 activation was investigated *via* luciferase reporter assay. BA strongly inhibited the activities of NF-κB and AP-1 (Fig. 4A). BA also decreased the expression of SOD2, one of NF-κB targets, and c-FOS, one of the major components of AP-1 at both mRNA and protein levels (Fig. 4B−D). The effect of BA on the phosphorylation of IκBα, p65 and MAPKs was investigated to ascertain the role of BA in regulating the activity of NF-κB and AP-1. BA significantly inhibited the phosphorylation of IκBα, p65, JNK, ERK and P38 in a time-course experiment (Fig. 4E and G). BA also attenuated p65 nuclear translocation (Fig. 4F). Investigation of the effect of individual inhibitors on RANKL-induced IL-1β expression suggested that IL-1β expression was significantly

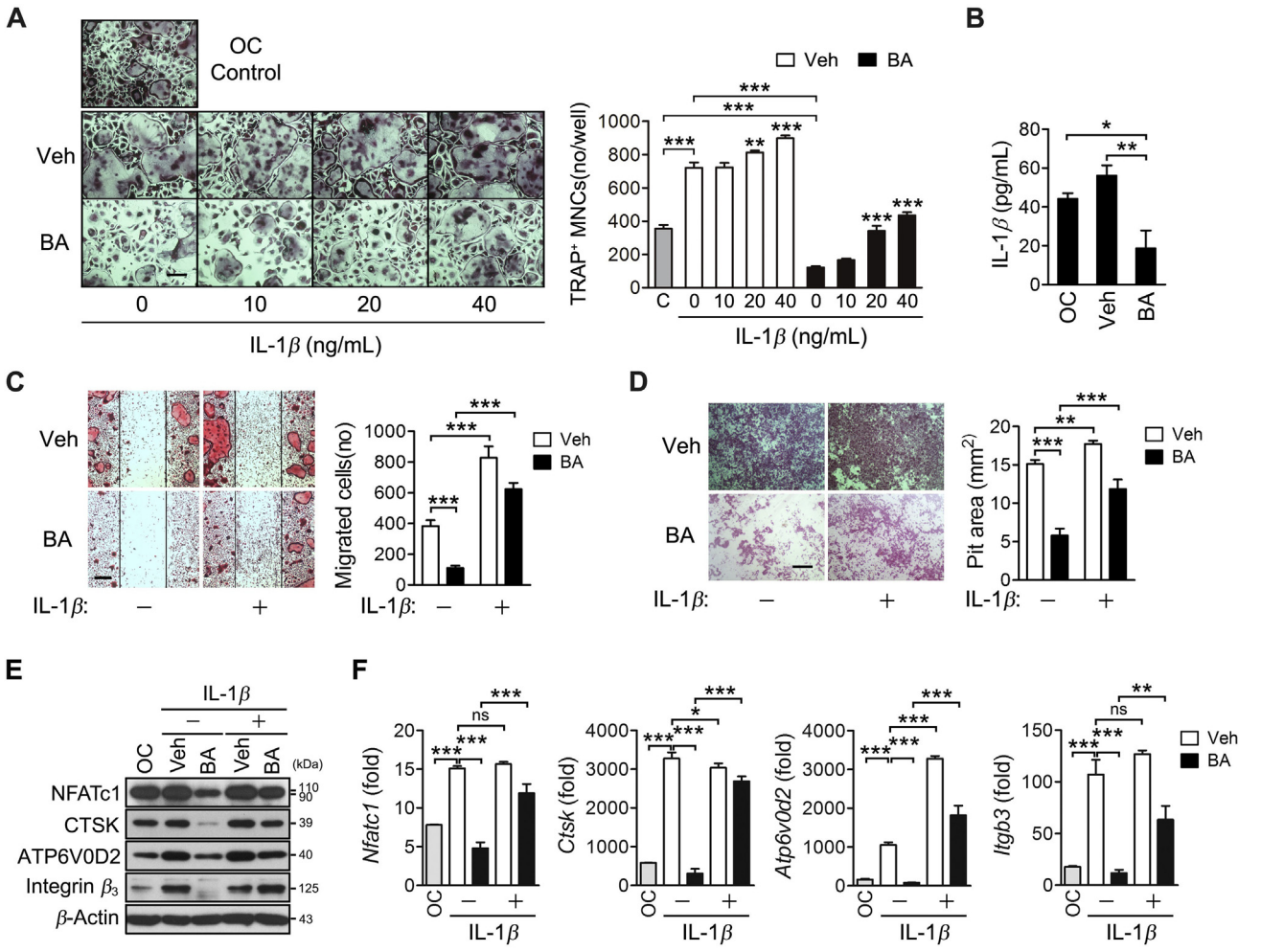

Figure 6 BA inhibition of differentiation, migration and bone resorption in osteoclasts, which was reversed by IL-1β treatment. BMMs were differentiated into osteoclasts *via* incubation with M-CSF and RANKL for 3 days, and the osteoclasts were incubated with BA in the absence or presence of IL-1β. (A) The cells were incubated with 10 μmol/L BA in the presence of IL-1β at the indicated concentrations for 2 days and subjected to TRAP staining. Scale bar, 200 μm. TRAP-positive MNCs were counted. (B) The cells were treated with 10 μmol/L BA for 2 days, and the amount of IL-1β in the culture media was determined by ELISA. (C) The cells were further incubated with 10 μmol/L BA in the absence or presence of IL-1β (20 ng/mL) for 15 h after gentle scratching and the cells migrating to the scratched area were counted. Scale bar, 200 μm. (D—F) The cells were cultured for 12 days on dentin discs (D) or 2 days (E and F) in the absence or presence of 10 μmol/L BA and IL-1β (20 ng/mL). The resorption pits were visualized by staining with hematoxylin (D). Cell lysates were subjected to immunoblotting analysis (E). The individual gene transcription was quantified by real-time PCR and presented as fold induction (F). Scale bar, 200 μm $^{*}P < 0.05$, $^{**}P < 0.01$ and $^{***}P < 0.001$ control *vs.* IL-1β in the absence and presence of BA (A), or between the indicated groups (A—D and E). ns, not significant.

decreased by IKKβ, ERK and P38 inhibitors, but not by JNK inhibitor (Fig. 4H). Collectively, these results indicate that BA inhibits the NF-κB and AP-1-dependent IL-1β expression *via* down-regulation of IKK, ERK and P38.

3.5. BA inhibits the migration and bone resorption, which is rescued by IL-1β treatment

The effects of BA and IL-1β on migration and bone resorption were explored. BA inhibited the migration whereas IL-1β promoted it; however, BA inhibition of migration was reversed by IL-1β (Fig. 5A). BA also inhibited bone resorption in the dentin disc and IL-1β completely restored the bone resorption suppressed by BA (Fig. 5B). In addition, the expression of osteoclast-specific genes including *Ctsk*, *Atp6v0d2,* and *Itgb3,* was inhibited by BA, and the inhibition was significantly reversed by IL-1β treatment (Fig. 5C and D). Together, BA appears to inhibit osteoclast differentiation, migration and bone resorption by suppressing IL-1β expression.

3.6. BA inhibits the maturation and resorption of differentiated osteoclasts, which is reversed by IL-1β

The IL-1β transcription was strongly induced in the later stages than in the early stage of osteoclastogenesis (Fig. 2). Thus, the effects of BA on osteoclast formation, migration, bone resorption, and osteoclast-specific gene expression in differentiated osteoclasts were also investigated. When BMMs were differentiated into osteoclasts by incubating with RANKL for 3 days followed by BA treatment, BA significantly inhibited osteoclast formation,

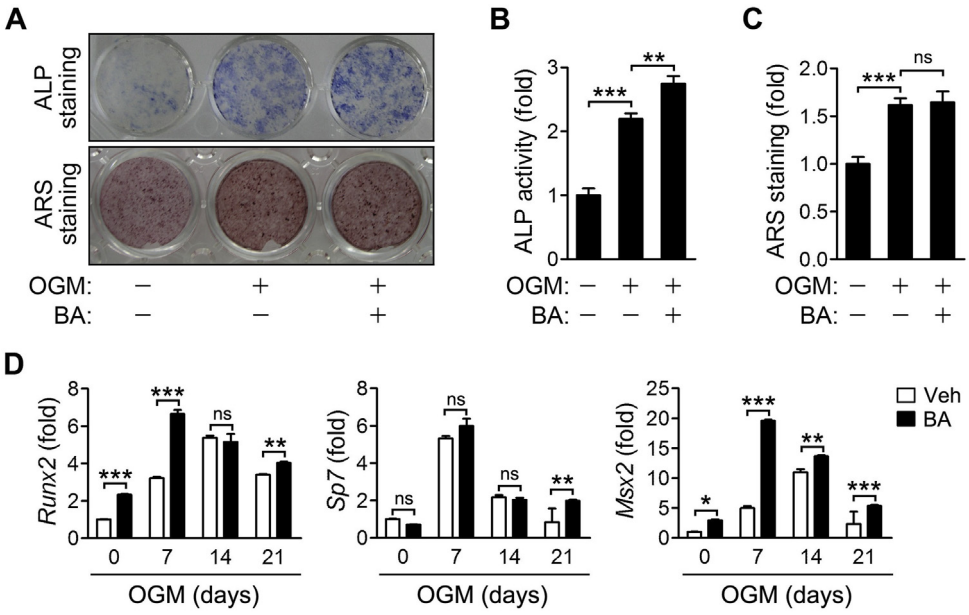

Figure 7 Effects of BA on osteoblast differentiation and mineralization. Calvaria cells were cultured in OGM for 12 days (A-upper panel and B), 21 days (A-lower panel and C) or the indicated times (D). (A) The cells were fixed in 4% paraformaldehyde and stained for ALP (upper panel) or with ARS (lower panel). (B) Cell lysates were subjected to ALP activity assay. (C) The ARS bound to cells was dissolved and the released ARS was measured. (D) The individual gene transcription was quantified by real-time PCR and presented as fold induction. $^{*}P < 0.05$, $^{**}P < 0.01$ and $^{***}P < 0.001$ between the indicated groups. ns, not significant.

which was effectively rescued by IL-1β treatment (Fig. 6A). BA decreased the amount of IL-1β secreted by the osteoclasts into culture media (Fig. 6B). In addition, BA inhibited the migration, bone resorption and osteoclast-specific gene expression in differentiated osteoclasts, all of which were reversed by IL-1β treatment (Fig. 6C–F). These results indicate that BA inhibited osteoclast maturation and function by suppressing IL-1β production.

3.7. *BA promotes osteoblast differentiation in vitro*

The effect of BA on osteoblast differentiation and function was also explored. Calvaria cells cultured in osteogenic media containing BA for 12 days were stained for the ALP activity. ALP-positive cells and ALP activity were increased by BA (Fig. 7A, upper panel and Fig. 7B). Also, the mRNA levels of transcription factors that regulate the expression of osteogenic genes were elevated in the BA-treated cells compared with vehicle-treated control cells (Fig. 7D). But, BA had no effect on the capacity to form mineralization bone nodules as indicated by ARS staining following 21 days differentiation under osteogenic condition (Fig. 7A, lower panel and Fig. 7C). Thus, these results demonstrate that BA enhances osteoblast differentiation but not mineralization.

3.8. *BA prevents bone loss induced by inflammation and ovariectomy*

The effect of BA on pathologic osteoclast formation and bone destruction was investigated using a model of inflammation-induced osteoclast formation and bone destruction, in which LPS was injected into the calvaria of mice. As shown in the TRAP staining analysis of whole calvaria and histology specimens, LPS increased the area of bone cavity and the number of TRAP-positive osteoclasts, which were significantly reduced by BA treatment (Fig. 8A–C). This result suggests that BA prevents inflammation-induced bone disease. Next, the therapeutic potential of BA was also evaluated using an OVX-induced model of postmenopausal osteoporosis. Histologic analysis of tibias from model mice showed that BA reduces TRAP-positive cells increased by OVX (Fig. 8D and E). Also, histomorphometric analyses of femurs of these mice revealed that OVX decreased the bone mineral density, bone surface, trabecular bone number and bone volume, and increased the trabecular pattern factor and trabecular separation (Fig. 8F and G). All these effects of OVX were significantly reversed by BA treatment, indicating the therapeutic potential of BA for the treatment of bone diseases such as osteoporosis.

4. Discussion

This study demonstrated that BA inhibited osteoclast differentiation and resorption *via* suppression of NF-κB or AP-1-dependent IL-1β production by regulating IKK, ERK and P38 activities. BA also enhanced osteoblast differentiation and prevented bone loss in inflammation- and OVX-induced bone destruction mouse models, demonstrating the role of BA as a novel drug for the treatment of bone diseases.

BA has been known to inhibit the production of pro-inflammatory cytokines including IL-1β, IL-6 and TNFα, and prostaglandin in several inflammatory conditions[26,32]. During osteoclastogenesis, RANKL induces a robust expression of IL-1β during both early and late stages, and a moderate expression of IL-6 in late stages. However, no expression of TNFα was induced. BA appears to inhibit IL-1β more effectively than IL-6 based on the induction fold. The IL-1β protein secreted into the media was also increased by RANKL and the increase was reversed by BA.

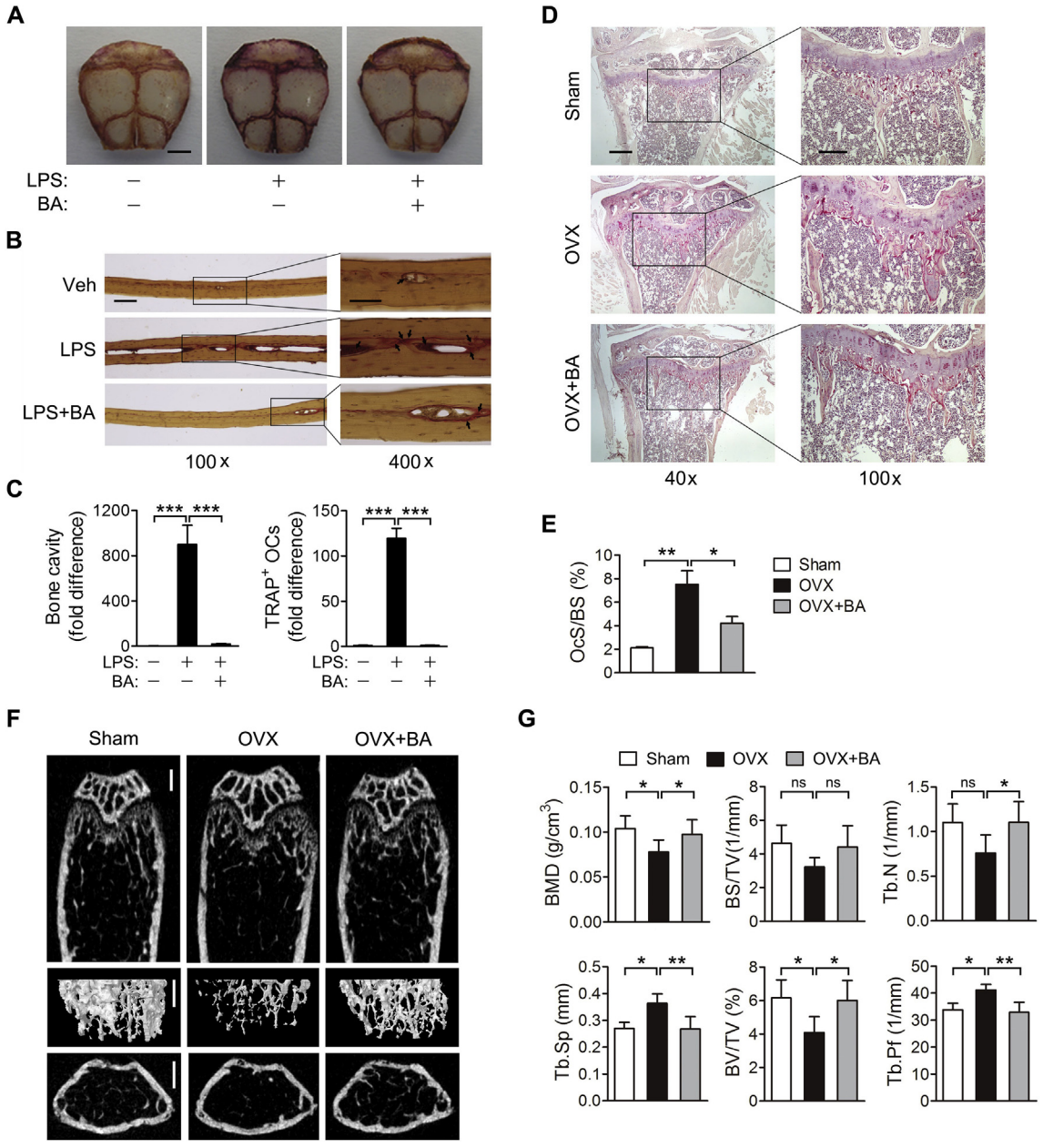

Figure 8 Inhibition of LPS- or OVX-induced bone destruction by BA. (A−C) LPS (12.5 mg/kg body weight) alone or with BA (10 mg/kg), each in a 100-μL volume of vehicle (PBS), was injected into the space between the subcutaneous tissue and the periosteum in the skulls of mice at days 0 and 2. Five days after first injection, the calvariae of mice were fixed, stained with TRAP and decalcified. (A) Images of TRAP and hematoxylin-stained calvaria. Scale bar, 2 mm. (B) The calvaria was embedded in paraffin, sectioned and stained with TRAP and hematoxylin. TRAP-positive cells are marked by arrow. Scale bar: 100 ×, 100 μm; 400 ×, 50 μm. (C) Bone cavity (left panel) and TRAP-positive osteoclasts (right panel) were quantified and expressed as fold difference. (D−G) Mice underwent either sham operation or OVX, and BA (10 mg/kg) was administrated to a group of mice intraperitoneally six times a week for three weeks. Sections of tibia were stained with TRAP and hematoxylin. Scale bar: 40 × , 100 μm; 100 × , 50 μm (D). The regions of TRAP-positive cells below the growth plate were measured. OcS/BS, osteoclast surface to bone surface (E). Representative micro-CT images of femurs: upper, sagittal; middle, three-dimensional reconstruction; bottom, transaxial; Scale bar, 0.5 mm (F). Histomorphometric analysis of femurs: BMD, bone mineral density; BS/TV, bone surface density; BS/BV, bone surface to bone volume; Tb.N, trabecular number; Tb.Th, trabecular thickness; BV/TV, bone volume density; Tb.Pf, trabecular pattern factor; Tb.Sp, trabecular spacing (G). $n = 5$. $^{*}P < 0.05$, $^{**}P < 0.01$ and $^{***}P < 0.001$ between the indicated groups. ns, not significant.

Prostaglandin is a fatty acid derivative[33], and therefore, its levels are very difficult to measure directly. Thus, the prostaglandin production was determined indirectly by quantifying the mRNA expression of prostaglandin synthesis-related enzymes including *Pla2*, *Cox2* and *Ptges*[34]. The enzyme expression was moderately induced by RANKL, and the induction was attenuated by BA. However, current results suggest that IL-1β is a major cytokine, which is strongly induced by RANKL and predominantly regulated by BA. Indeed, the treatment of IL-1β with RANKL promoted osteoclast differentiation and reversed the inhibitory effects

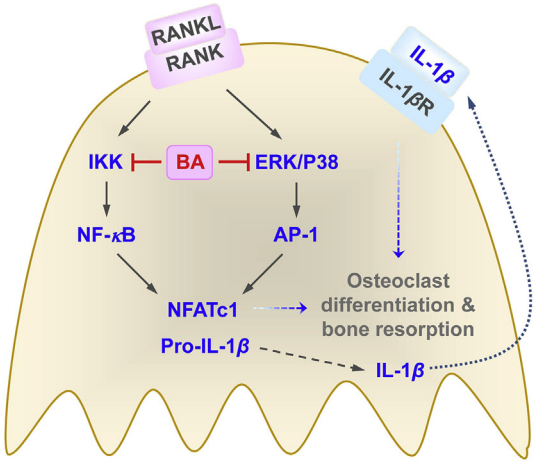

Figure 9 The proposed mechanism of BA inhibition of osteoclast differentiation and bone resorption *via* down-regulation of IL-1β and NFATc1 expression.

of BA; however, PGE2 treatment marginally affected the inhibitory effects of BA. In addition, IL-1β treatment completely reversed the migration and bone resorption that was suppressed by BA. Therefore, BA appears to inhibit osteoclast differentiation and bone resorption *via* down-regulation of IL-1β production.

The expression of IL-1β is regulated by NF-κB and AP-1[30,31]. BA inhibited RANKL-induced activation of NF-κB and AP-1 promoter, suggesting that BA suppresses IL-1β expression *via* inhibition of NF-κB and AP-1. BA inhibited IκBα phosphorylation and p65 nuclear translocation, and IKKβ inhibitor decreased IL-1β expression. Thus, BA appears to suppress NF-κB-dependent IL-1β expression by inhibiting IKK activity. BA also inhibited RANKL-induced c-FOS expression and MAPKs activation. The RANKL-induced IL-1β expression was inhibited by ERK and P38 inhibitors, but not by JNK inhibitor. The expression of c-FOS, a major component of AP-1, is regulated by ELK-1, serum response factor (SRF) and cAMP response element-binding protein[35]. *c-Fos* and *Elk-1* were identified as downstream target genes of NF-κB[36,37], indicating that NF-κB regulates AP-1 activity. The phosphorylation of ELK-1 occurs primarily *via* ERK[38–40], although the phosphorylation may also be mediated by JNK and P38, depending on the stimuli[41]. ERK is also reported to increase *c-Fos* expression *via* phosphorylation of SRF[42]. The RANKL-induced *c-Fos* induction is down-regulated by P38 inhibitors[43]. Thus, it might be speculated that BA regulates RANKL-induced IKK, ERK and P38 activation, leading to the suppression of IL-1β expression *via* down-regulation of NF-κB and AP-1.

IL-1β is expressed in a proform (pro-IL-1β), which is converted to a mature form through inflammasome-mediated caspase-1 activation, and then secreted. BA strongly decreased the transcription of IL-1β and also significantly reduced the amount of secreted IL-1β protein. However, the inhibition fold of IL-1β secretion was not higher than that of IL-1β transcription. Thus, BA inhibition of IL-1β production may occur primarily in the transcription level, although the possibility of BA to affect inflammasome could not be completely excluded. IL-1β is an osteoclastogenic cytokine, which enhances osteoclast differentiation and bone resorption activity[21,22]. It was recently reported that the addition of IL-1β in the presence of M-CSF and RANKL induces pathological activated osteoclasts having extremely high levels of resorbing activity[44]. Taken together, BA may inhibit NF-κB and AP-1 through down-regulation of IKK, ERK and P38, leading to the suppression of IL-1β and NFATc1 expression, resulting in the inhibition of osteoclast differentiation and bone resorption (Fig. 9).

To test the usefulness of BA for treating bone diseases triggered by excessive osteoclastic activity, its effects on differentiated osteoclasts were also investigated. BA effectively inhibited the formation, migration and bone resorption of osteoclasts, and its inhibitory effects were reversed by IL-1β treatment. These results suggest that BA could inhibit the maturation and bone resorption of differentiated osteoclasts. BA also promoted osteoblast differentiation, though the underlying mechanism remains to be elucidated. IL-1 deficient mice exhibited reduced osteoclast differentiation and increased bone density and trabecular bone mass[45], suggesting that IL-1 plays an important role in the bone homeostasis and IL-1 blockade might have therapeutic implication. The therapeutic potential of BA to treat pathological bone diseases was evaluated in mouse models of both LPS-induced and OVX-mediated bone destruction. BA has been administered orally or subcutaneously at 10 or 20 mg/kg in mouse models, respectively[46,47]. Therefore, BA was used at a dose of 10 mg/kg (calvarial or intraperitoneal injection) in the present study. Our results suggest that BA plays a potential therapeutic role in the treatment of inflammation-induced bone diseases and postmenopausal osteoporosis.

5. Conclusions

BA inhibits osteoclast differentiation and resorption by suppressing IL-1β synthesis *via* down-regulation of IKK, ERK and P38, and promotes osteoblast differentiation. BA is an FDA-approved drug, and the protective role of BA against inflammation-mediated bone loss and menopause-induced osteoporosis in mouse models reinforces the clinical role of BA as a novel therapeutic agent against pathologic bone diseases.

Acknowledgments

This work was supported by the National Research Foundation (NRF) (Grant Nos. 2017R1A2B2012435, 2019R1C1C1011198 and 2019R1A5A6099645, Korea) funded by the Korean Ministry of Science, ICT and future Planning (MSIP).

Author contributions

Han Saem Son and Jiae Lee conducted most of the research and wrote the manuscript; Hye In Lee, Narae Kim, You-Jin Jo, Seong-Eun Hong, Minjung Kwon, Nam Young Kim, Hyun Jin Kim and Jin Ha Park helped with the experiment; Gong-Rak Lee and Soo Young Lee participated in discussions; and Woojin Jeong guided the entire study and edited the manuscript.

Conflicts of interest

The authors declare that they have no conflict of interest.

References

1. Arron JR, Choi Y. Bone *versus* immune system. *Nature* 2000;**408**:535−6.
2. Phan TC, Xu J, Zheng MH. Interaction between osteoblast and osteoclast: impact in bone disease. *Histol Histopathol* 2004;**19**:1325−44.
3. Abe T, Shin J, Hosur K, Udey MC, Chavakis T, Hajishengallis G. Regulation of osteoclast homeostasis and inflammatory bone loss by MFG-E8. *J Immunol* 2014;**193**:1383−91.
4. Hirayama T, Danks L, Sabokbar A, Athanasou NA. Osteoclast formation and activity in the pathogenesis of osteoporosis in rheumatoid arthritis. *Rheumatology* 2002;**41**:1232−9.
5. Hong SE, Lee J, Seo DH, In Lee H, Park DR, Lee GR, et al. Euphorbia factor L1 inhibits osteoclastogenesis by regulating cellular redox status and induces Fas-mediated apoptosis in osteoclast. *Free Radic Biol Med* 2017;**112**:191−9.
6. Lee J, Son HS, Lee HI, Lee GR, Jo YJ, Hong SE, et al. Skullcapflavone II inhibits osteoclastogenesis by regulating reactive oxygen species and attenuates the survival and resorption function of osteoclasts by modulating integrin signaling. *FASEB J* 2019;**33**:2026−36.
7. Lee HI, Lee J, Hwang D, Lee GR, Kim N, Kwon M, et al. Dehydrocostus lactone suppresses osteoclast differentiation by regulating NFATc1 and inhibits osteoclast activation through modulating migration and lysosome function. *FASEB J* 2019;**33**:9685−94.
8. Boyce BF, Xing L. Functions of RANKL/RANK/OPG in bone modeling and remodeling. *Arch Biochem Biophys* 2008;**473**:139−46.
9. Arch RHGR, Thompson CB. Tumor necrosis factor receptor-associated factors (TRAFs)—a family of adapter proteins that regulates life and death. *Genes Dev* 1998:2821−30.
10. Asagiri M, Takayanagi H. The molecular understanding of osteoclast differentiation. *Bone* 2007;**40**:251−64.
11. Johnson GL, Lapadat R. Mitogen-activated protein kinase pathways mediated by erk, jnk, and p38 protein kinases. *Science* 2002;**298**:1911−2.
12. Teitelbaum SL, Ross FP. Genetic regulation of osteoclast development and function. *Nat Rev Genet* 2003;**4**:638−49.
13. Boyce BF, Yamashita T, Yao Z, Zhang Q, Li F, Xing L. Roles for NF-kappa B and c-Fos in osteoclasts. *J Bone Miner Metab* 2005;**23**:11−5.
14. Wagner EF, Eferl R. Fos/AP-1 proteins in bone and the immune system. *Immunol Rev* 2005;**208**:126−40.
15. Asagiri M, Sato K, Usami T, Ochi S, Nishina H, Yoshida H, et al. Autoamplification of NFATc1 expression determines its essential role in bone homeostasis. *J Exp Med* 2005;**202**:1261−9.
16. Takayanagi H. The role of NFAT in osteoclast formation. *Ann N Y Acad Sci* 2007;**1116**:227−37.
17. Boyle WJ, Simonet WS, Lacey DL. Osteoclast differentiation and activation. *Nature* 2003;**423**:337−42.
18. Pahl HL. Activators and target genes of Rel/NF-kappaB transcription factors. *Oncogene* 1999;**18**:6853−66.
19. Ricciotti EFG. Prostaglandins and inflammation. *Arterioscler Thromb Vasc Biol* 2011;**31**:986−1000.
20. Dinarello CA. Proinflammatory cytokines. *Chest* 2000;**118**:503−8.
21. Nakamura I, Jimi E. Regulation of osteoclast differentiation and function by interleukin-1. *Vitam Horm* 2006;**74**:357−70.
22. Ruscitti PCP, Carubbi F, Liakouli V, Zazzeroni F, Di Benedetto P, Berardicurti O, et al. The role of il-1β in the bone loss during rheumatic diseases. *Mediat Inflamm* 2015;**2015**:782382.
23. Manolagas JR SC. Bone marrow, cytokines, and bone remodeling. Emerging insights into the pathophysiology of osteoporosis. *N Engl J Med* 1995;**332**:305−11.
24. Kobayashi YMT, Take I, Kurihara S, Udagawa N, Takahashi N. Prostaglandin E2 enhances osteoclastic differentiation of precursor cells through protein kinase A-dependent phosphorylation of TAK1. *J Biol Chem* 2005;**280**:11395−403.
25. Cioli V, Corradino C, Scorza Barcellona P. Review of pharmacological data on benzydamine. *Int J Tissue React* 1985;**7**:205−13.
26. Segre G, Hammarstrom S. Aspects of the mechanisms of action of benzydamine. *Int J Tissue React* 1985;**7**:187−93.
27. Jin SH, Kim H, Gu DR, Park KH, Lee YR, Choi Y, et al. Actin-binding LIM protein 1 regulates receptor activator of NF-kappa B ligand-mediated osteoclast differentiation and motility. *BMB Rep* 2018;**51**:356−61.
28. Kim H, Hyeon S, Kim H, Yang Y, Huh JY, Park DR, et al. Dynein light chain LC8 inhibits osteoclast differentiation and prevents bone loss in mice. *J Immunol* 2013;**190**:1312−8.
29. Zhang Y, Rom WN. Regulation of the interleukin-1 beta (IL-1 beta) gene by mycobacterial components and lipopolysaccharide is mediated by two nuclear factor-IL6 motifs. *Mol Cell Biol* 1993;**13**:3831−7.
30. Cogswell JP, Godlevski MM, Wisely GB, Clay WC, Leesnitzer LM, Ways JP, et al. NF-kappa B regulates IL-1 beta transcription through a consensus NF-kappa B binding site and a nonconsensus cre-like site. *J Immunol* 1994;**153**:712−23.
31. Serkkola E, Hurme M. Synergism between protein-kinase C and cAMP-dependent pathways in the expression of the interleukin-1 beta gene is mediated *via* the activator-protein-1 (AP-1) enhancer activity. *Eur J Biochem* 1993;**213**:243−9.
32. Sironi M, Milanese C, Vecchi A, Polenzani L, Guglielmotti A, Coletta I, et al. Benzydamine inhibits the release of tumor necrosis factor-alpha and monocyte chemotactic protein-1 by candida albicans-stimulated human peripheral blood cells. *Int J Clin Lab Res* 1997;**27**:118−22.
33. Hansen HS. Essential fatty acid supplemented diet increases renal excretion of prostaglandin E2 and water in essential fatty acid deficient rats. *Lipids* 1981;**16**:849−54.
34. Murakami M, Naraba H, Tanioka T, Semmyo N, Nakatani Y, Kojima F, et al. Regulation of prostaglandin E2 biosynthesis by inducible membrane-associated prostaglandin E2 synthase that acts in concert with cyclooxygenase-2. *J Biol Chem* 2000;**275**:32783−92.
35. Hazzalin CA, Mahadevan LC. MAPK-regulated transcription: a continuously variable gene switch?. *Nat Rev Mol Cell Biol* 2002;**3**:30−40.
36. Tu YC, Huang DY, Shiah SG, Wang JS, Lin WW. Regulation of c-Fos gene expression by NF-kappaB: a p65 homodimer binding site in mouse embryonic fibroblasts but not human HEK293 cells. *PLoS One* 2013;**8**:e84062.
37. Fujioka S, Niu J, Schmidt C, Sclabas GM, Peng B, Uwagawa T, et al. NF-kappa B and AP-1 connection: mechanism of NF-kappa B -dependent regulation of AP-1 activity. *Mol Cell Biol* 2004;**24**:7806−19.
38. Gille H, Kortenjann M, Thomae O, Moomaw C, Slaughter C, Cobb MH, et al. ERK phosphorylation potentiates ELK-1-mediated ternary complex formation and transactivation. *EMBO J* 1995;**14**:951−62.
39. Whitmarsh AJ, Shore P, Sharrocks AD, Davis RJ. Integration of MAP kinase signal transduction pathways at the serum response element. *Science* 1995;**269**:403−7.
40. Wang Y, Prywes R. Activation of the c-Fos enhancer by the ERK MAP kinase pathway through two sequence elements: the c-Fos AP-1 and p62TCF sites. *Oncogene* 2000;**19**:1379−85.
41. Whitmarsh AJ, Yang SH, Su MS, Sharrocks AD, Davis RJ. Role of p38 and JNK mitogen-activated protein kinases in the activation of ternary complex factors. *Mol Cell Biol* 1997;**17**:2360−71.
42. Eto K, Hommyo A, Yonemitsu R, Abe S. ErbB4 signals neuregulin1-stimulated cell proliferation and c-fos gene expression through phosphorylation of serum response factor by mitogen-activated protein kinase cascade. *Mol Cell Biochem* 2010;**339**:119−25.
43. Huang H, Chang EJ, Ryu J, Lee ZH, Lee Y, Kim HH. Induction of c-Fos and NFATC1 during rankl-stimulated osteoclast differentiation is mediated by the p38 signaling pathway. *Biochem Biophys Res Commun* 2006;**351**:99−105.

44. Shiratori T, Kyumoto-Nakamura Y, Kukita A, Uehara N, Zhang J, Koda K, et al. IL-1beta induces pathologically activated osteoclasts bearing extremely high levels of resorbing activity: a possible pathological subpopulation of osteoclasts, accompanied by suppressed expression of kindlin-3 and talin-1. *J Immunol* 2018;**200**:218−28.
45. Lee YM, Fujikado N, Manaka H, Yasuda H, Iwakura Y. IL-1 plays an important role in the bone metabolism under physiological conditions. *Int Immunol* 2010;**22**:805−16.
46. Yamazaki-Nishioka M, Shimizu M, Suemizu H, Nishiwaki M, Mitsui M, Yamazaki H. Human plasma metabolic profiles of benzydamine, a flavin-containing monooxygenase probe substrate, simulated with pharmacokinetic data from control and humanized-liver mice. *Xenobiotica* 2018;**48**:117−23.
47. Guglielmotti A, Aquilini L, Rosignoli MT, Landolfi C, Soldo L, Coletta I, et al. Benzydamine protection in a mouse model of endotoxemia. *Inflamm Res* 1997;**46**:332−5.